HEFAT2010
7th International Conference on Heat Transfer, Fluid Mechanics and Thermodynamics
19-21 July 2010
Antalya, Turkey

CFD ANALYSIS OF TURBULENT FORCED CONVECTION IN A PLANE CHANNEL WITH A BUILT-IN TRIANGULAR PRISM

[1]Benim A.C*, [2]Chattopadhyay,, H., [1]Nahavandi, A. and [1,3]Ozer C.
*Author for correspondence
[1]Department of Mechanical and Process Engineering,
Duesseldorf University of Applied Sciences,
Josef-Gockeln-Str. 9, D-40474 Duesseldorf,
Germany,
E-mail: alicemal.benim@fh-duesseldorf.de
[2]Department of Mechanical Engineering,
Jadavpur University,
Kolkata - 700032,
India,
[3]Department of Mechanical Engineering,
Sakarya University,
Sakarya,
Turkey.

ABSTRACT

Turbulent forced convection in a heated two-dimensional channel with a centrally built-in prism with a triangular cross section is computationally investigated by different turbulence modelling strategies. These include Reynolds Averaged Numerical Simulations (RANS), Unsteady RANS (URANS) and Large Eddy Simulations (LES). RANS and two-dimensional URANS (2D URANS) are performed for a range of Reynolds numbers (Re) extending from 2,500 to 250,000. The Prandtl number is kept at the value of 0.7 (corresponding to air) in all computations. Three dimensional URANS (3D URANS), as well as LES (which are by definition three-dimensional) are additionally performed for Re = 2,500. In RANS and URANS, the Shear Stress Transport (SST) model is employed as the turbulence model. It is shown that the heat transfer at channel walls can be augmented by presence of the triangular prism, and the prediction quality depends on the modelling approach applied in the analysis. It is demonstrated that the effect of the unsteady motion of the coherent vortex structures behind the prism are mainly responsible for the heat transfer augmentation, and their influence cannot adequately be represented by RANS, calling for an unsteady approach, such as URANS or LES. The comparison between the predictions of 2D URANS and 3D URANS as well as LES shows, on the other hand, that this flow unsteadiness is also intimately related with flow three-dimensionality, as the time-averaged Nusselt numbers vary depending on the dimensionality assumed.

INTRODUCTION

Heat transfer augmentation is an important research field, as it enables savings in energy and costs [1], and, being so, has continuously been the subject of a large amount of theoretical, experimental and computational investigations, so far.

In different engineering disciplines, there exist numerous applications of heat transfer in channels. Thus, for heat transfer augmentation in channels, different geometric arrangements such as vortex generators, e.g. in the form of delta wing or winglet pair or by insertion of twisted tapes have been used. Furthermore, flow around bluff bodies such as a round cylinder or a square cylinder has also been investigated. Influence of the presence of obstacles with different shapes was investigated e.g. by Jackson [2] via Finite Element Method (FEM) simulations for laminar flow.

A prism element with a triangular cross section is a basic configuration. However, its role has not yet been analysed in sufficient detail. Abbasi et al. [3] showed that use of such an obstacle could enhance the heat transfer in a plane channel. However, their numerical analysis based on FEM was limited to the laminar flow regime. In their analysis [3], they demonstrated that a considerable heat transfer enhancement can be achieved by incorporating a triangular prism. An important flow characteristics enhancing the heat transfer was found, here, to be the periodic occurrence of vortices behind triangular prism (as it is generally the case for any bluff body) that enhance the mixing and heat transfer [4].

Recently, Chattopadhyay [5] presented a numerical analysis of a geometrical configuration that is very similar to the one used by Abbasi et al. [3], for the turbulent flow regime. In the work of Chattopadhyay [5], a steady-state analysis was applied, within the framework of a RANS (Reynolds Averaged Numerical Simulations) [6] formulation of the turbulent flow. Within a RANS formulation, the periodic vortex shedding behind the triangular prism, which has already been mentioned, above, to be the main source of the heat transfer augmentation [3], can, of course, not be resolved in time. Within RANS, one needs to assume that the consequences of the unsteady motion onto the time-averaged fields get properly represented by the applied RANS turbulence model. However, as already demonstrated in different applications, this assumption is not necessarily valid. For the unconfined flow around a circular cylinder, e.g., it was shown [7] that the time-averaged drag force predicted by RANS may be largely in error, where more accurate predictions could be obtained by a URANS or an LES formulation that resolve the unsteadiness of the fluid motion. For the present problem, one can similarly expect that the unsteady nature of the vortical flow behind the triangular prism, which could not directly be resolved with the RANS formulation of [5], plays also a role for the time-averaged heat transfer characteristics. This point makes up the main focus of the present study.

In the present investigation, a further improvement of the investigation presented in [5] is aimed, where the role of the unsteady phenomena is considered to be the main emphasis. The unsteady motion of turbulent vortical structures is, in general, intimately related with flow three-dimensionality. Thus, the role of a three-dimensional modelling in combination with an unsteady approach is also investigated.

NOMENCLATURE

B	[m]	Base of triangular prism cross section
c	[-]	Dimensionless speed (nondim. by inlet speed)
c_p	[J/kgK]	Isobaric specific heat capacity
D_h	[m]	Hydraulic diameter
H	[m]	Channel height
h	[W/m^{2}K]	Heat transfer coefficient ($h=q/(T_W-T_{F,0})$)
k	[W/mK]	Thermal conductivity
k	[m^2/s^2]	Turbulence kinetic energy
Nu	[-]	Nusselt number ($Nu=hD_h/k$)
Pr	[-]	Prandtl number ($Pr=\mu c_p/k$)
q	[W/m^2]	Heat flux
Re	[-]	Reynolds Number ($Re=\rho u_0 D_h/\mu$)
T	[K]	Temperature
u	[m/s]	Axial velocity
y^+	[-]	Dimensionless wall distance ($y^+=(y/\delta)(\tau_w/\rho)^{0.5}$)

Greek symbols

δ	[m]	Distance of next-to-wall cell to wall
ε	[m^2/s^3]	Dissipation rate of turbulence kinetic energy
θ	[-]	Dimensionless temperature ($\theta=(T-T_{F,0})/(T_W-T_{F,0})$)
μ	[Pa.s]	Dynamic viscosity
ν	[m^2/s]	Kinematic viscosity
ρ	[kg/m^3]	Density
τ_w	[Pa]	Wall shear stress

Subscripts

F	Fluid
W	Wall
0	Inlet

MODELLING

Incompressible, turbulent, non-isothermal flow of a Newtonian fluid is analysed for different Re, keeping Pr=0.7. The computational analysis is performed using the general purpose CFD code ANSYS Fluent [8]. For RANS and URANS analysis, the Shear Stress Transport (SST) turbulence model [9] is employed. In the past investigations on turbulent forced convection [10], a satisfactory performance of this model was observed. A major purpose of the present work is the analysis of the unsteady phenomena. Thus, an important, additional reason for using this turbulence model is its ability of capturing unsteady phenomena [7], within the framework of a URANS formulation, provided that no wall-functions approach [8,11] is used, and the near-wall layer is resolved sufficiently. Thus, the SST turbulence model [8,9] is used in RANS and URANS computations, without employing wall-functions. Alternative turbulence models such as the k-ε model [8,11] have been observed not to capture flow unsteadiness at all (if the boundary conditions are in steady-state), with or even without using wall-functions, their unsteady computations (URANS) converging to a steady-state solution. Additionally, an LES [12] formulation is applied, utilizing the Wall-Adapting Local Eddy Viscosity Model (WALE) [13] as the subgrid-scale model. In the LES investigations, too, the near-wall layer is resolved sufficiently fine, without using the wall-functions.

In the LES analysis, the convective terms of the momentum equations are discretized by the central differencing scheme [6,8], whereas the high resolution scheme [14] is used for the energy equation, to preserve boundedness. In the RANS and URANS analysis, the high resolution scheme is used for discretizing all convection terms. For treating the pressure, the SIMPLEC [15] algorithm is used for the steady-state computations, whereas the PISO [16] algorithm is employed for the unsteady simulations. In all unsteady calculations, a second order backward Euler scheme [8] is applied to discretize the governing equations in time. In all simulations, Fluent's default under-relaxation coefficients are employed (1.0, for pressure and temperature, 0.7 for velocity, and 0.8 for turbulence quantities). Normalized residuals required for fulfilling the convergence criteria has been set to 10^{-8} for the energy, and 10^{-5} for the remaining equations. These values correspond to 1% of Fluent's default tolerance values [6]. In the unsteady computations, for time-accuracy, the time step size is always chosen in such a way that the condition of Co < 1 is satisfied, where Co denotes the cell Courant number [6]. A flow integral time scale T_I, can be defined as the ratio of the channel height to inlet bulk velocity ($T_I = H / u_0$). The employed computational time step sizes (Δt) varied between approx. 4.0×10^{-3} T_I and 1.5×10^{-4} T_I (corresponding to 2.5×10^{-4} s and 1.0×10^{-5} s) from case to case. The time step size is additionally controlled in comparison to the physical time scales. In all cases, the employed time step sizes have been at least of similar order to the Kolmogorov time scale [12]. Thus, a satisfactory resolution of physical time scales throughout can be assumed. Transient computations are performed, first, for a long enough time period for a periodic flow pattern to develop. After reaching of this state, the time-averaging is initiated. The time averaging is performed until obtaining time-independent time-averaged results.

RESULTS

Preliminary Investigation

Before analyzing the main problem, steady-state turbulent forced convection in a 2D, simple channel "without any triangular prism" has been investigated, for gaining more confidence in the applied modelling strategy. Here, the predicted Nusselt numbers are compared with the empirical information provided by the Dittus-Boelter equation [17]:

$$\mathrm{Nu} = 0.023\ \mathrm{Pr}^{0.4}\ \mathrm{Re}^{0.8} \qquad (1)$$

This equation is known to be valid for Re > 10,000. Thus, the comparison is done for a Reynolds number in this range, i. e. for Re = 250,000. For this comparison, a channel length of about 60 D_h is considered, for assuring aerodynamically and thermally fully-developed conditions in the outlet section of the channel, where the comparison with the empirical expression (Eq. (1)) is performed. It may be noteed that the heat transfer coefficient (h) used to compute Nu in this comparison is based on the temperature difference between the local mean fluid temperature (T_F) (averaged over the channel-cross section) and the wall temperature (T_W) ($h = q / (T_W-T_F)$), as required by the definitions behind Eq. (1). A structured grid with rather low expansion ratios is generated, which leads to grid independent results and fulfill the condition of $y^+ < 1$ for the near-wall cells. Table I compares the empirical Nusselt number with the predicted one. The percentage deviation of the values is also shown in the table.

As one can see from Table I, the agreement between the predictions and the empirical value is quite good (Table I). In a similar study performed previously [18] concerning a circular pipe flow (but, for different values of Re) a quite good general agreement was also observed, using similar modelling strategies [18]. We assume that the results for a circular pipe may show an even better agreement to the empirical equation, since the representation of the present planar channel flow by an equivalent hydraulic diameter (D_h=2H) may be causing an additional uncertainty in the usage of Eq. (1) that was originally based on a circular pipe.

Geometry, Boundary Conditions

The configuration of Abbasi et al. [3] is also considered in the present investigation, for the turbulent flow. The two-dimensional flow domain in and the boundary types are shown in Figure 1. Boundaries of the blocks to generate the block-structured grids are also indicated in the figure.

For 3D URANS and LES, the depth of the domain is assumed to be equal to the channel height (H). On the boundaries in the third dimension, periodic boundary conditions are applied. Thus, the aim, here, is not the computation of a real 3D geometry (e.g. channel with square cross-section). Three-dimensionality is introduced for being able to cope with the 3D URANS and LES modelling of

Table I Empirical and predicted Nusselt numbers for channel flow, for Re = 250 000.

	Empirical	Predicted	Deviation
Nu	415.1	426.6	+ 3 %

turbulence, where the time-averaged flow field still remains two-dimensional. A channel depth of H equals four times the base (B, Fig. 1) of the triangular prism cross section. It cannot be claimed, of course, in advance, that this depth is large enough to allow three-dimensional structures to get freely formed without substantial interferences with the bounding planes in the third direction. However, in similar investigations out of the open literature, e.g. for the aerodynamics of the flow past an unconfined circular cylinder, using transient, three-dimensional procedures, such as LES, it is quite often found to be sufficient to choose the depth of the domain to be about three times the cylinder diameter [19] (which can be taken to be comparable to the base of the triangle). Thus, based on this comparison, the present domain depth may be assumed to be large enough.

At the inlet, spatially uniform and temporally constant velocity and temperature profiles are prescribed as boundary conditions. Inlet boundary conditions for the turbulence quantities are derived assuming a macro length-scale of 30 % of the hydraulic diameter and a turbulent intensity of 4%. For the LES computations no flow disturbances are prescribed at the inlet. At the outlet, a constant static pressure is prescribed together with zero-gradient conditions for the remaining variables. At the walls, no-slip conditions apply. For the energy equation, a spatially and temporally constant temperature is applied at the non-adiabatic channel walls. The walls of triangular prism are assumed to be adiabatic.

Grids

Block-structured grids with conformal block interfaces are used (grid block boundaries are also shown in Fig. 1). For an adequate resolution of the near-wall layer in turbulent flow, it is always guaranteed that the condition of $y^+ < 1$ fulfilled. Using rather mild geometric expansion ratios (normally always smaller than 1.15), boundary layers are resolved with higher resolution. This ensures that the laminar sub-layer, i.e. the near-wall region with $y^+ < 5$ is resolved by at least about 4 cells.

Grid independency is tested within the framework of 2D, steady-state, RANS formulations. Steady-state solutions, i.e. RANS results can be obtained, if only half the domain is considered, by introducing an artificial symmetry plane through the channel mid-height, i.e. through the middle of the prism, since the symmetry plane artificially suppresses the unsteady vortex shedding associated with the physical problem. It may be noted that this is true if SST is used as turbulence model, resolving the near-wall layers (no wall-functions). If wall-functions are used (in combination with SST), or if a k-ε model

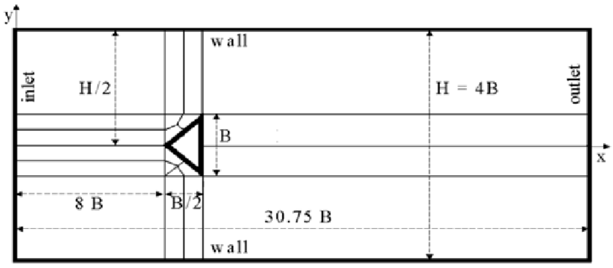

Figure 1 Geometry, block structure, boundary types.

is used (with or without using wall-functions), a flow unsteadiness could not be captured, results converging to steady-state solutions (RANS), although the full domain (Fig. 1) (no artificial symmetry plane) was considered and an unsteady solution procedure (URANS) was applied.

In the following, the sizes of the "almost"-structured grids shall be indicated by the number of cells in x and y directions, where, N_x denotes the number of cells along the channel wall, and N_y the number of the cells along the channel inlet. Since the grid has a locally unstructured configuration in the vicinity of the prism (Fig.1), the total number of resulting cells is slightly different from the multiplication of N_x and N_y.

Grids assuring a grid independent solution in RANS are taken as basis for the unsteady computations (URANS, LES), by mirroring them around the symmetry plane used in RANS. The 3D grid, for 3D URANS and LES is generated by "extruding" the 2D URANS grid (x-y plane) in the third direction (z direction). For the grid resolution in the third direction, no additional grid independency study is performed. Since the main shearing of the flow occurs primarily in the x-y plane, it is assumed that the structures occurring in the perpendicular plane (y-z plane) will not necessarily be finer than those of the x-y plane. Thus, it is assumed that it would provide a sufficient resolution, if the resolution in the z-direction is made comparable to that of the y-direction Therefore, since the domain depth is equal to the height, the number of cells in the z direction are set to be equal to the number of cells in the y direction (N_z=N_y). The cells in the third (z) direction are, however, distributed equidistantly, where the distribution in the y direction is non-uniform for resolving wall boundary layers.

Table II presents the applied grid resolutions for Re = 2,500 and Re = 250,000, within the framework of 2D URANS. In RANS, the size is halved (by halving N_y, since half the domain is considered). In 3D URANS or LES, the 3D grid is structured to have N_z = N_y. A detail view of the grid for Re = 250,000, used for RANS (half domain) is shown in Figure 2. For LES, the resolution of turbulent scales by the grid is checked by an additional parameter. In [20], it was demonstrated that a very good, i.e. "DNS like" accuracy can be achieved in LES, if the ratio of the grid size to the Kolmogorov length scale [12] is about 5 to 10. For the present analysis, the maximum value of this ratio within the whole domain, turned out to be about 9, where the mean value was about 4, indicating a quite good accuracy for the LES computations of Re = 2,500, as far as this aspect is concerned.

Velocity fields

Contours of dimensionless speed at a time-step predicted by 2D URANS are presented in Figure 3, for Re=250,000. Vortex structures behind the prism can be observed in the figure. Figure 4 compares the time-averaged velocity field obtained by 2D URANS, with the results of a RANS computation. The RANS computation is performed in half domain, using an artificial symmetry plane (for enforcing a steady-state solution),

Table II Grids for 2D URANS (size indicated by $N_x \times N_y$)

Re = 2,500	Re = 250,000
80 x 74	178 x 353

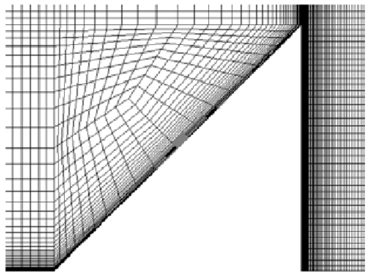

Figure 2 Detail view of RANS grid for Re = 250,000.

as already discussed above. One can observe that both velocity fields show substantial differences. For example, the recirculation zone behind the prism is predicted much longer in the RANS computation, compared to the time-averaged 2D URANS predictions (Fig. 4). Similar discrepancies are observed for different Reynolds numbers. This shows the inappropriateness of the steady-state, i.e. RANS modelling in such flows. It should also be mentioned that k-ε results (without wall-functions, resolving near-wall layers, applied under 2D URANS and using full-domain) that converge to steady-state solutions are similar to those of the present RANS (Fig. 4b).

In 3D URANS and LES, the so-called Q-criterion [21] is

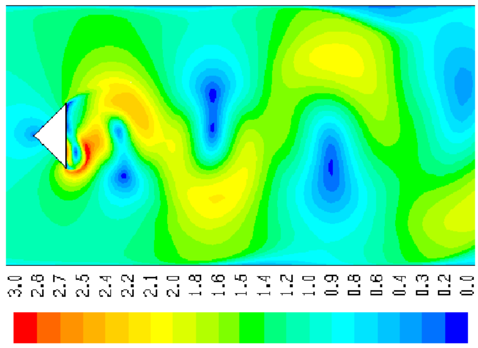

Figure 3 Dim.-less speed (c) at a time step, Re=250,000.

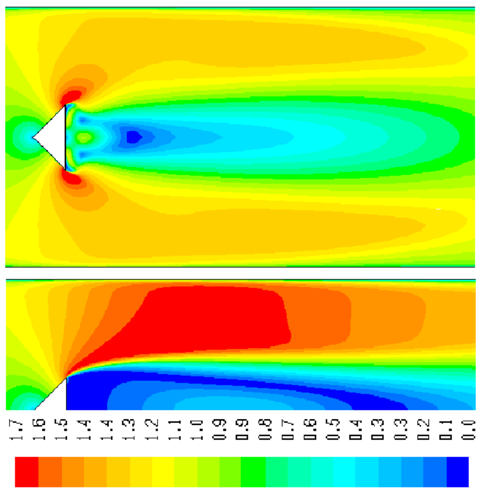

Figure 4 Dimensionless speed (c) for Re=250,000, top: time-averaged URANS, bottom: RANS.

used to capture the vortical structures. Figure 5 shows the predicted iso-surfaces, for a time-step, Q = 100 $1/s^2$, as predicted by 3D URANS and LES. For 3D URANS, one can see that some three-dimensional structures are additionally captured, although a rather two-dimensional character is still predominant (Fig. 5a). In LES, one can observe that much finer structures are captured compared to 3D URANS, which also exhibit a much stronger three-dimensional structure (Fig. 5b).

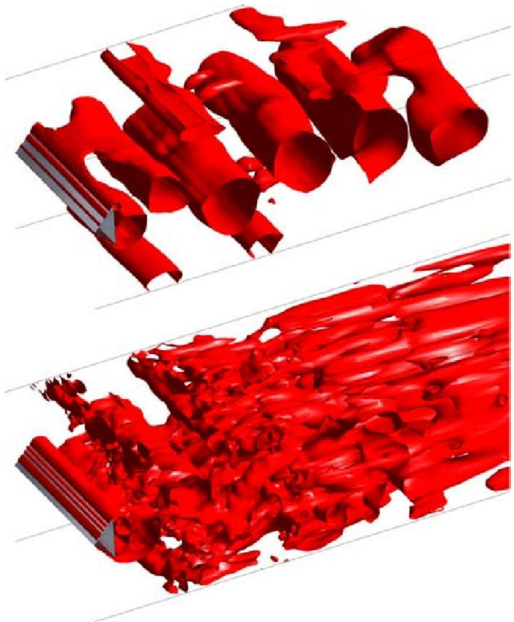

Figure 5 Q=100 s^{-2} isosurfaces at a time-step, for Re=2,500, top: 3D URANS, bottom: LES.

Temperature fields

Dimensionless temperature contours are presented in Figure 6, for Re=250,000. In the figure, the predictions for the simple channel without a prism (RANS) are also shown. One can see the disturbance of the thermal boundary layer by the unsteady-periodic flow (Fig. 6a), which causes a thickening of the thermal boundary layer in time-average (Fig. 6b) compared to the undisturbed channel flow, without prism (Fig. 6c).

Isosurfaces of the dimensionless temperature (θ) predicted by 3D URANS and LES, for Re=2,500, at a time-step, are displayed in Figure 7, for θ=0.5. The three-dimensional structures can of course be observed in the temperature field, of course. 3D URANS exhibit a three-dimensionality that rather increases within a range in the wake region. The structures resolved by LES are even finer, as one would expect (Fig. 7).

Heat transfer

Predicted Nusselt number variations along the channel wall, for Re=2,500 and Re=250,00, are shown in Figure 8 and Figure 9, respectively. For URANS and LES, the time-averaged results are shown. One can see that the prediction strongly depends on the modelling applied. One can observe that maximum Nu predicted by URANS and LES occurs at a farther downstream position compared to RANS, and the enhancement does not

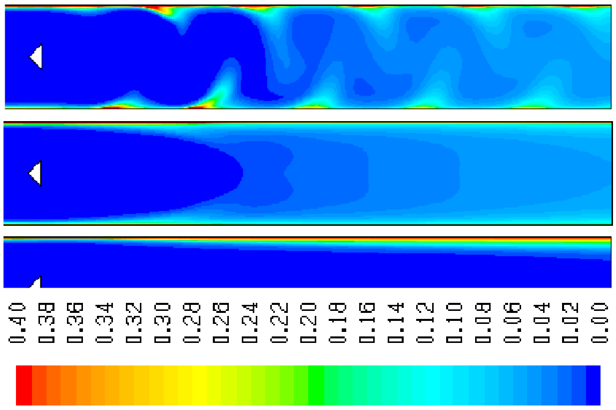

Figure 6 Dimensionless temperature (θ) for Re=250,000, top: URANS at a time-step, middle: URANS time-averaged, bottom: RANS

Figure 7 θ=0.5 isosurfaces at a time-step, for Re=2,500, top: 3D URANS, bottom: LES.

rapidly decay behind the prism, but lasts for the whole channel. Although the peak Nu value predicted by RANS, for Re=2,500, is even higher than that of URANS, the Nu values in the wake region are underpredicted by RANS, leading to an underprediction of the overall heat transfer. These comparisons show the important role of the flow unsteadiness for heat transfer enhancement, especially in the wake region. One can also see that flow three-dimensionality plays also an important role, as 3D URANS results predict generally higher values than 2D URANS. It is interesting to note that LES predict a remarkably higher Nu peak value than 3D URANS.

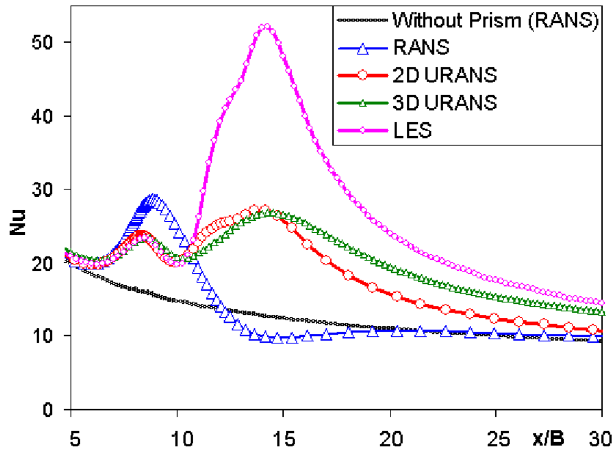

Figure 8 Predicted Nu along channel wall, Re=2,500.

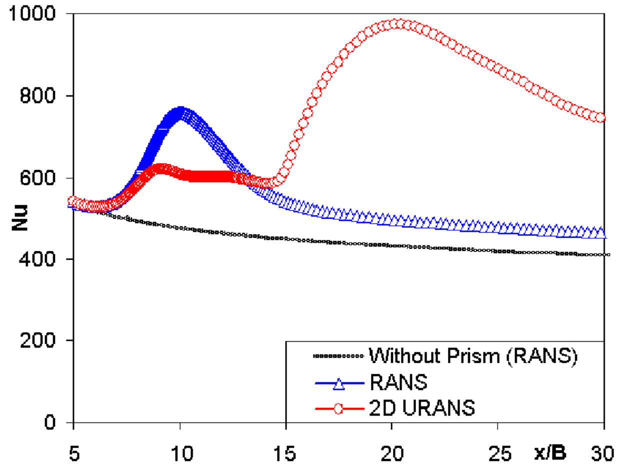

Figure 9 Predicted Nu along channel wall, Re=250,000.

CONCLUSION

Turbulent forced convection in a two-dimensional channel with a triangular prism has been computationally investigated for different Reynolds numbers, for Prandtl number of 0.7. It has been shown that heat transfer to channel walls can be augmented by the triangular prism. Comparing 2D URANS and RANS, it has additionally been demonstrated that a modelling approach that cannot capture flow unsteadiness underpredicts (time-averaged) the heat transfer enhancement. In 3D URANS computations for Re=2,500, it has been shown that the coherent vortex structures are not perfectly two-dimensional, but also exhibit a certain three-dimensionality. Finer, turbulent three-dimensional structures are resolved, of course, by LES. As far as the time-averaged Nusselt numbers at channel walls are concerned, an additional influence of flow three-dimensionality has been observed, that leads to higher Nusselt numbers, (3D URANS and LES results) for Re=2,500. It is interesting to note that the LES predicts a considerably higher peak value for the Nusselt number, compared to 3D URANS. Further analysis of turbulence models will be the subject of the future work.

REFERENCES

[1] Bejan, A. E., Techniques to augment heat transfer, in: *Handbook of Heat Transfer Applications*, McGraw-Hill, New York, 1983, pp. 31-80.

[2] Jackson, C. P., A finite element study of the onset of vortex shedding in flow past variously shaped bluff bodies, *Journal of Fluid Mech*anics, Vol. 363, 1987, pp. 23-45.

[3] Abbasi, H., Turki, S. and Ben Nasrallah, S., Numerical investigation of forced convection in a horizontal channel with a built-in triangular prism, *ASME Journal of. Heat Transfer*, Vol. 124, 2002, pp. 571-573.

[4] Biswas, G. and Chattopadhyay, H., Heat transfer in a channel with built-in wing type vortex generators, *International Journal of Heat and Mass Transfer*, Vol. 35, 1992, pp. 803-814.

[5] Chattopadhyay, H., Augmentation of heat transfer in a channel using a triangular prism, *International. Journal of Thermal Sciences*, Vol. 6, 2007, pp. 501-505.

[6] Peyret, R. *Handbook of Computational Fluid Mechanics*, Academic Press, San Diego, 1996.

[7] Benim, A. C., Pasqualotto, E. and Suh, S. H., Modelling turbulent flow past a circular cylinder by RANS, URANS, LES and DES, *Progress in Computational Fluid Dynamics*, Vol. 8, 2008, pp. 299-307.

[8] Fluent 6.3, *User's Guide*, Fluent Inc., Lebanon, NH, 2009.

[9] Menter, F. R., Zonal two equation k-ω turbulence models for aerodynamic flows, *AIAA Paper 93-2906*, 1993.

[10] Benim, A. C., Ozkan, K., Cagan, M. and Gunes, D., Computational investigation of turbulent jet impinging onto rotating disk, *International Journal for Numerical Methods in Heat and Fluid Flow,* Vol. 17, 2007, pp. 284-301.

[11] Launder, B. E. and Spalding, D. B., The numerical computation of turbulent flows, *Computer Methods in Applied Mechanics and Engineering*, Vol. 3, 1974, pp. 269-289.

[12] Sagaut, P., *Large eddy simulation for incompressible flows – an introduction*, 2nd Ed. Springer, Berlin, 2002.

[13] Nicoud F. and Ducros, F., Subgrid-scale stress modelling based on the square of the velocity gradient tensor, *Flow, Turbulence, and Combustion*, Vol. 62, 1999, pp. 183-200.

[14] Barth, T. J. and Jespersen, D., The design and application of upwind schemes on unstructured meshes, *Technical Report AIAA-89-0366*, 1989.

[15] Vandoormaal J. P. and Raithby, G. D. Enhancements of the SIMPLE method for predicting incompressible fluid flows, *Numerical Heat Transfer*, Vol. 7, 1984, pp. 147-163.

[16] Issa, I. R., Solution of implicitly discretized fluid flow equations by operator splitting, *Journal of Computational Physics*, Vol. 62, 1985, pp. 40-65.

[17] Baehr, H. D. and Stephan, K., *Wärme- und Stoffübertragung,* Springer, Berlin, 1994.

[18] Benim, A. C., Cagan, M. and Gunes, D., Computational analysis of transient heat transfer in turbulent pipe flow, *International Journal of Thermal Sciences,* Vol. 43, pp. 2004, pp. 725-732.

[19] Breuer, M., Large eddy simulations of the subcritical flow past a circular cylinder: numerical and modelling aspects, *International Journal for Numerical Methods in Fluids*, Vol. 28, 1988, pp. 1281-1302.

[20] Fröhlich, J., Mellen, C. P., Rodi, W., Temmerman, L. and Leschziner, M. A., Higly resolved large-eddy simulation of separated flow in a channel with periodic constrictions, *Journal of Fluid Mechanics*, Vol. 526, 2005, 19-66.

[21] Hunt, J. C. R., Wray, A. A. and Moin, P. Eddies, Stream and Convergence Zones in Turbulent Flows, *Report CTR-S88*, Center for Turbulence Research, Stanford University, 1988.